

# Performance of an SIS receiver over 460 GHz to 640 GHz using submicron Nb junctions with integrated RF tuning circuits

P. Febvre<sup>1</sup>, W.R. McGrath, P. Batelaan, H.G. LeDuc, B. Bumble, M.A. Frerking, J. Hernichel<sup>2</sup>

Jet Propulsion Laboratory, California Institute of Technology, Pasadena, CA 91109  
1. Permanent address: DEMIRM-Observatoire de Meudon, 92195 Meudon Cedex, France  
2. Permanent address: Universität Köln, 5000 Köln 41, Germany

## ABSTRACT

A heterodyne receiver using an SIS waveguide mixer with two mechanical tuners has been characterized from 460 GHz to 640 GHz. The mixer uses submicron Nb/AlO<sub>x</sub>/Nb SIS tunnel junctions with integrated superconductive RF circuits to tune the junction capacitance. DSB receiver noise temperatures as low as 200''+ 17 K at 540 GHz and  $362 \pm 33$  K at 626 GHz have been obtained which are among the best results reported to date in this frequency range. In addition, negative differential resistance has been observed in the DC I-V curve at 487-49 GHz.

## 1. INTRODUCTION

The most sensitive heterodyne receivers used for millimeter wave and submillimeter wave radioastronomy employ superconductor-insulator-superconductor (SIS) tunnel junctions as the nonlinear mixing element. Good performance has recently been reported for SIS junctions used in planar mixer circuits [1, 2] and waveguide mixers [3-8] from about 300 GHz to 500 GHz. In general, however, few SIS mixers have been demonstrated at these high frequencies. We have developed a submillimeter wave SIS heterodyne receiver for observing important rotational transitions of molecules in the

interstellar medium, and in particular the ground state transitions of  $\text{H}_2^{18}\text{O}$  at 547 GHz and  $\text{HCl}$  at 626 GHz. This receiver is based on a waveguide mixer with an adjustable backshort and E-plane tuner [9]. The mixer uses a high current density, submicron area  $\text{Nb-AlO}_x\text{-Nb}$  tunnel junction. The large capacitive susceptance of the junction at high frequencies will shunt the signal away from the nonlinear conductance and hence must be properly tuned for optimum performance. This is accomplished here through the use of carefully designed superconductive microstrip circuits to match the complex impedance of the junction to the available tuning range of the waveguide mount. The receiver performance has been measured over the frequency range 460 GHz to 640 GHz. DSB receiver noise temperatures as low as  $200 \pm 17$  K at 540 GHz and  $362 \pm 33$  K at 626 GHz have been obtained, and are among the best values reported to date at this frequency. In addition, negative differential resistance has been observed in the DC I-V curve at frequencies around 491 GHz. These results indicate that the superconductive Nb microstrip transmission lines used in the tuning circuits are low-loss and perform well up to at least 90% of the superconductor energy gap frequency.

## II. SIS JUNCTIONS WITH INTEGRATED TUNING CIRCUITS

High quality  $\text{Nb-AlO}_x\text{-Nb}$  tunnel junctions have been fabricated using a trilayer deposition and self-aligned insulator lift-off process [10]. The junction area of  $0.25 \mu\text{m}^2$  is defined by electron beam lithography, while the junction leads and RF filter circuit are produced by conventional photolithography. The Nb films are DC sputter deposited. The base electrode is  $1600 \text{ \AA}$  thick and the top electrode is  $2300 \text{ \AA}$ . The junctions have an estimated specific capacitance of  $85\text{-}100 \text{ fF}/\mu\text{m}^2$ , current densities in the range  $8,000\text{-}13,000 \text{ A}/\text{cm}^2$ , and normal state resistances  $R_N$  in the range  $60 \Omega\text{-}100 \Omega$ . The integrated RF tuning circuits are defined by the Nb wiring electrode on a  $2000 \text{ \AA}$  thick  $\text{SiO}$  insulating layer. Figure 4 shows a typical I-V curve.

The integrated RF tuning circuit that resonates the junction capacitance is a parallel microstrip line terminated in a radial stub as shown in Figure 1. This circuit has been designed for center frequencies near both 550 and 630 GHz. The radial stub is used to provide an RF short over a broad bandwidth. The stub dimensions were designed using an effective dielectric constant, which accounts for the penetration of the magnetic field into the superconductor. The short is then transformed to an inductance by an appropriate section of microstrip line to compensate the capacitance of the junction. The characteristic impedance  $Z_0$  of this line was chosen close to  $(2\pi f_s C_J)^{-1}$  to optimize the bandwidth ( $f_s$  is the signal frequency and  $C_J$  is the junction capacitance).

The superconducting microstrip line is a slow-wave line due to the penetration of the magnetic field into the Nb films over a distance comparable to the SiO<sub>2</sub> dielectric thickness. In order to properly design our microstrip circuits, the characteristic impedance  $Z_0$  and phase velocity  $v$  of the line must be known. These are given by  $Z_0 = \sqrt{L/C}$  and  $v = 1/\sqrt{LC}$  where  $L$  is the inductance per unit length of line and  $C$  is the capacitance per unit length. Convenient expressions [11, 12] valid below the gap frequency, are given by:

$$C = k\epsilon_r\epsilon_0 w/t_d \quad (1)$$

and

$$L = \frac{\mu_0}{kw} \left[ t_d + \lambda \left[ \coth(t_1/\lambda) + \coth(t_2/\lambda) \right] \right] \quad (2)$$

where  $w$  is the width of the microstrip,  $t_1$  and  $t_2$  are the thicknesses of the top and bottom Nb films respectively,  $t_d$  is the thickness of the SiO<sub>2</sub> insulating layer,  $\epsilon_r = 5.5$  is the dielectric constant of SiO<sub>2</sub>, and  $k$  is a fringing field factor.  $k$  varies between 1.05 and 1.37 as a function of the width of the line [13]. Equations (1) and (2) are valid for  $w/t_d \gg 1$ . A penetration depth  $\lambda = 750 \text{ \AA}$  [14] was used as the nominal value.

As indicated by both theory and experiment [14] (reference 14 contains an improved theoretical model of the dispersion in superconductive microstrip line which agrees well

with measurements), the dispersion and loss in these Nb transmission lines can be neglected in this application up to about 550-600 GHz. Thus we have not included these effects in our design. These circuits have been designed to resonate the junction capacitance based on a specific capacitance of  $85 \text{ fF}/\mu\text{m}^2$ . In addition a series microstrip transformer circuit has been designed [15] to resonate junction capacitances ranging from  $60 \text{ fF}/\mu\text{m}^2$  to  $100 \text{ fF}/\mu\text{m}^2$ ; a value which is dependent on the current density of the junction. A systematic study of mixer performance for these different circuits will be published at a later date.

### III. RECEIVER DESIGN AND MEASUREMENT TECHNIQUES

The SIS tunnel junction, integrated tuning circuit, and low-pass RF filter are fabricated on  $50 \mu\text{m}$  thick quartz which is cut to a width of  $150 \mu\text{m}$  for the 550 GHz RF filter and  $100 \mu\text{m}$  for the 630 GHz RF filter. This substrate is installed into the waveguide mixer mount and wire bonded to the  $50 \Omega$  IF output connector. The waveguide mixer was designed using a low-frequency model to maximize the accessible region of impedances on the Smith chart over an equivalent frequency range of 500 GHz to 600 GHz [9]. This mixer has an adjustable backshort and E-plane tuner which provide a wide range of impedances to the SIS junction. Radiation is coupled into the waveguide mount by a dual mode conical horn [16].

Figure 2 shows a block diagram of the receiver. The local oscillator (LO) source consists of two whisker-contacted Schottky varactor frequency multipliers ( $\times 2 \times 3$ ) [17] driven by a Gunn oscillator. We varied this Gunn oscillator frequency and used two other Gunn sources to make measurements in the 460 GHz to 630 GHz frequency range. The signal and LO are combined in a folded Fabry-Perot diplexer and injected into the cryostat through a differentially-pumped window using two  $125 \mu\text{m}$  thick mylar vacuum windows, Fluorogold far IR filters, one wavelength thick at 550 GHz, on the 77 K and 4 K stages, block room temperature radiation from saturating the mixer. An off-axis elliptical mirror

reflects the combined radiation into the mixer which is installed on the 4 K stage of the cryostat. The 1.4 GHz IF output of the mixer is transformed to the required  $50\ \Omega$  input impedance of the low noise HEMT amplifier by a 2 step Chebyscheff microstrip transformer made on 1.27 mm thick Duroid substrate with  $\epsilon_r = 10.5$ . The IF is further amplified by two high-gain room-temperature amplifiers. The band-width for noise measurements is 300 MHz. A superconducting magnet is used to suppress unwanted Josephson interference and thus improve receiver performance. It has been designed to provide a magnetic field of about 800 gauss near the junction for a current through the coil of 1 ampere. This is sufficient since 1 flux quantum in our junction corresponds to about 340 gauss.

The total receiver noise temperature is determined by the Y-factor method using hot (295 K) and cold (82 K) loads. The reference plane for these measurements is the input of the diplexer (see Figure 2). Since the Rayleigh-Jeans approximation of the Planck law is not valid in the frequency range of this receiver, the radiation power from the loads has been calculated using the full Planck expression. The classical formula  $P = kTB$  is replaced by  $P = hvB/(\exp(hv/kT)-1)$  where  $k$  is Boltzmann's constant and  $v$  is the LO frequency. However, the noise power per unit bandwidth of the receiver is expressed as a temperature using the classical expression.

## IV. RESULTS AND DISCUSSION

### A. Receiver performance

The receiver performance has been measured over an LO frequency range from 460 GHz to 640 GHz. One SIS junction with no RF integrated tuning circuit and two junctions with integrated circuits have been measured. Figure 3 shows the DSB receiver noise temperature as a function of the LO frequency. Junction A used a tuning circuit

designed to resonate the junction capacitance at 550 GHz, while the tuning circuit with junction B has been optimized for 630 GHz. For each data point in Figure 3, the waveguide backshort and E-plane tuner, LO level, and DC bias voltage were optimized. The best performance at 540 GHz was for junction A ( $R_N = 63 \Omega$ ) which gave  $T_R = 200 K$  (Y-factor = 1.78). The receiver was very good with this junction, yielding  $T_R \leq 300 K$  over the frequency range from 463 GHz to 549 GHz. The only exception was a few points near 490 GHz, where the noise increased due to the appearance of negative differential resistance (this is discussed in more detail below). Above 600 GHz the noise temperature increases rapidly with the frequency because the tuning circuit does not compensate completely the junction capacitance in this frequency range. The receiver performed well up to 635 GHz with junction B ( $R_N = 73 \Omega$ ) and gave a noise temperature of 362 K at 626 GHz. This second junction also exhibited a receiver noise temperature of 400-430 K in the range 530-550 GHz and 270 K at 490 GHz. The noise temperature of this junction increases in the range 460-490 GHz which may be due to an undesirable resonance of the low-pass RF filter caused by the substrate not working properly in the waveguide mount [9]. This is due to the width of the quartz substrate of junction B having been optimized for a mixer mount centered at 630 GHz but measured in a 550 GHz mixer mount.

An SIS junction without any tuning circuit has also been measured from 460 to 630 GHz. One can clearly see in Figure 3 that the high capacitance of the SIS junction is not completely compensated by the mechanical tuning backshorts. This is mostly due to the RF losses of the backshorts which limit the range of low impedances which can be provided to the junction. The DSB receiver noise temperature is 850-1150 K from 470 to 550 GHz. Under 470 and above 600 GHz the noise increases which may be due to the limitations of the mixer mount range of RF matching impedances. Further theoretical analysis of the mixer performance is required.

We also observed an increase of noise near 549-553 GHz which is due to the presence of a strong water line at 557 GHz. The line absorbs part of the signal coming from the cold load and emits at room-temperature. By putting the cold load at different positions: close to the Fabry-Perot diplexer and up to 9 cm away, a difference in the receiver temperature is clearly observed. From this increase of temperature, it is possible to determine the absorption due to the water line. An absorption of about 0.037 dB/cm at 549 GHz was deduced. This measured value is in reasonable agreement with the theoretically calculated absorption given the inaccuracy of the technique. Such an absorption can add at least 30 K at 549 GHz to the receiver temperature due to the signal path length up to the cryostat window. All junctions tested to date show some increase in the receiver temperature above about 549 GHz.

Figure 4 shows the unpumped and LO pumped I-V curves of junction A, which gave the best performance at 540 GHz. The unpumped curve shows very low subgap current and a sharp gap structure at 2.85 mV. The photon step is clearly seen on the pumped I-V curve. Also shown in this figure is the IF output power from the receiver for both hot and cold loads as broadband signal sources at the RF input. It can be seen that the IF power is low near zero voltage which indicates that the Josephson current has been almost completely suppressed with the magnetic field of the superconducting coil corresponding to about 2 flux quanta. In addition, there is a dip in the IF power curve near 1.5 mV which corresponds to a small variation in the slope of the pumped IV curve, but it does not create any noticeable additive noise at the operating bias voltage at about 2 mV.

#### B. Negative differential resistance

A DC negative differential resistance has been observed on the 1st photon step at LO frequencies of 487 GHz and 491 GHz with junction A. This is a quantum mechanical effect which is not predicted by classical theory. Also, negative resistance implies that the

available mixer gain can be infinite in theory. When the mixer is biased in the negative resistance region, the IF output power is very high and unstable, probably due to low frequency oscillations. As a result, the receiver is unstable and noisier at these frequencies. However, since the negative resistance did not extend completely across the photon step, it was possible to bias the junction at these frequencies though not at an optimum point. As seen in Figure 3, the receiver noise is higher by 100 K -200 K in this region.

The negative resistance at 491 GHz could not be eliminated by adjusting the backshort and E-plane tuner. This indicated that the microstrip tuning circuit was very strongly coupled to the junction and had at least fully compensated the junction capacitance as well as providing a susceptance necessary for negative resistance. Also, the microstrip losses must be very low. A similar result has been previously reported at 230 GHz [18]. The LO source does not cover the range 500-520 GHz, so the full bandwidth over which this tuning circuit resonates well is not known. This circuit was nominally designed for 550 GHz. This result shows that it actually resonates at a lower frequency than expected (in agreement with Josephson resonances, as discussed below).

### C. Tuning circuit resonances

The superconducting tuning circuits were designed to resonate the junction capacitance near 550 GHz and 630 GHz. However, resonant peaks in the DC I-V curve suggest the circuits resonate at lower frequencies. That is, an S1S junction biased at a voltage  $V$ , produces a high frequency oscillation given by  $f = 484 \text{ GHz} \times V \text{ (mV)}$  due to the AC Josephson effect. Generally, at high frequencies, the capacitance of the junction shunts these oscillations. But at the frequencies where the tuning circuit resonates the capacitance i.e. at the DC voltages corresponding to these frequencies, these Josephson oscillations interact with the non-linear resistance of the S IS junction and give a DC current peak on the I-V curve [19,20]. Peaks were observed at about 1.08 mV, corresponding to



520 GHz, for junction A and at about 1.20 mV, corresponding to 580 GHz for junction B. This suggests that the parameters chosen for the calculation of the superconducting microstrip lines are not exactly right: the penetration depth of the Nb films may be higher and/or the specific capacitance of these high current-density SIS junctions has been underestimated.

#### D. Mixer noise temperature and conversion efficiency

The shot-noise produced by the linear resistance of the SIS junction I-V curve for voltages higher than the gap voltage was used to calibrate the IF system. This is a simple technique to calibrate the IF system noise and gain, thus allowing the mixer noise and conversion efficiency to be estimated from the measured receiver performance. The SIS junction acts as a variable temperature load when the junction is biased on the linear part of its I-V curve. The IF system output power as a function of this temperature is a straight line: its slope is the gain of the IF system and the temperature at zero IF power is the IF system noise. From this calibration, junction A which exhibited 200 K noise temperature at 540 GHz, has a mixer DSB noise temperature of about 180 K with a coupled conversion efficiency (including the IF mismatch) of about -6 dB. Junction B which gave 362 K at 626 GHz has a mixer noise temperature of about 270 K and a coupled conversion efficiency of about -12 dB. In both cases the largest contribution to the receiver noise comes from the mixer noise. The mixer noise includes the RF mismatch as well as the losses in the optics, the windows and the Fabry-Perot.

### V. CONCLUSION

A receiver for radioastronomy applications in the range 460-640 GHz has been demonstrated. The best results are a DSB receiver temperature as low as 200 K at 540 GHz

and 362 K at 626 GHz. The optics have been designed to work in the 500-600 GHz RF frequency range. Nevertheless, this receiver was tested at lower and higher frequencies to determine the behavior of the integrated tuning circuits which resonate with the SIS junction capacitance. A differential negative resistance has been observed at 487 GHz and 491 GHz which indicates that the circuits work better at frequencies lower than designed. This is also confirmed by the resonances resulting from the AC Josephson current and observed on the unpumped I-V curves.

In addition, we have begun measuring the performance of this receiver using a series array of two junctions made by optical lithography techniques [21]. A noise temperature  $T_R(\text{DSB}) = 330$  K has so far been achieved at 49 GHz. This work is in progress and will be reported later.

#### ACKNOWLEDGEMENTS

We wish to acknowledge the fabrication of the array junctions by P. Feautrier and the contribution of T. Kuiper for calculating the theoretical atmosphere water line absorption near 550 GHz. This work was supported in part by the Jet Propulsion Laboratory, California Institute of Technology, under contract to the National Aeronautics and Space Administration and the Innovative Science and Technology Office of the Strategic Defense Initiative Organization. Pascal Febvre has been partly sponsored by Matra Marconi Space, Toulouse, France and the DEMIRM (Département de Radioastronomie Millimétrique), Observatoire de Meudon, France.

## REFERENCES

- [1] J. Zmuidzinas and H.G. LeDuc, "Quasioptical slot antenna SIS mixers," IEEE Trans. Microwave Theory Tech., vol. 40, N09, pp 1797-1804, September 1992.
- [2] T.H. Büttgenbach, H.G. LeDuc, P.D. Maker and T.G. Phillips, "A fixed tuned broadband matching structure for submillimeter SIS receivers," IEEE Trans. Appl. Superconductivity, vol. 2, pp 165-175, September 1992.
- [3] G. de Lange, C.E. Honingh, M. M.T. M. Dierichs, R.A. Panhuyzen, H.H.A. Schaeffer, T.M. Klapwijk, H. van de Stadt, M.W.M. de Graauw, "A low noise 410-495 Heterodyne two tuner mixer using submicron Nb/Al<sub>2</sub>O<sub>3</sub>/Nb tunnel junctions," Proceedings of the 3rd Int'l Symp. Space Terahertz Tech., pp. 210-221, Ann Arbor, MI, March 24-26, 1992.
- [4] C.K. Walker, J.W. Kooi, M. Chant, H.G. LeDuc, P.L. Schaffer, J.E. Carlstrom, and T.G. Phillips, "A low noise 492 GHz SIS waveguide receiver," Int. J. IR mm Waves, vol. 13, No. 6, pp. 785-798, 1992.
- [5] P. Febvre, P. Feautrier, C. Robert, J.C. Pernot, A. Germont, M. Hanus, R. Maoi, M. Gheudin, G. Beaudin, P. Encrenaz, "A 380 GHz SIS Receiver using Nb/AlOx/Nb junctions for a radioastronomical balloon-borne experiment: PRONAS," Proceedings 3rd Int'l Symp. Space Terahertz Tech., pp. 189-209, Ann Arbor, MI, March 24-26, 1992.
- [6] B.N. Ellison, P.L. Schaffer, W. Schaal, D. Vail and R.E. Miller, "A 345 GHz SIS receiver for radioastronomy," Int. J. IR mm Waves Vol. 10, No. 8, 1989.

- [7] A. Karpov, M. Carter, B. Lazareff, M. Voss, D. Billon-Pierron, K. H. Gundlach,  
"The 350 GHz and 230 GHz mixers with the tuned SIS junctions," Conference  
Digest of the 17th Int'l Conf. on IR and mm Waves, pp. 340-341, California Institute  
of Technology, Pasadena, California, December 14-17, 1992.
  
- [8] C.E. Honingh, G. de Lange, M. M.T.M. Dierichs, H.H.A. Schaeffer, J. Wezelman,  
J. v.d. Kuur, Th. de Graauw and T.M. Klapwijk, "Comparison of Measured and  
Predicted Performance of a SIS Waveguide Mixer at 345 GHz," Proceedings of the  
3rd Int'l Symp. on Space Terahertz Tech., pp. 251-265, Ann Arbor, MI, March 24-  
26, 1992.
  
- [9] W.R. McGrath, K. Jacobs, J. Stern, H.G. LeDuc, R.E. Miller, M.A. Frerking,  
"Development of a 600- to 700-GHz SIS receiver, " Proceedings of the 1st Int'l  
Symposium on Space Terahertz Technology, pp. 409-433, Ann Arbor, MI, March 5-  
6, 1990.
  
- [10] H.G. LeDuc, B. Bumble, S.R. Cypher, A.J. Judas, J.A. Stern, "Submicron area  
Nb/AlOx/Nb tunnel junctions for submillimeter mixer applications," Proceedings of  
the 3rd Int'l Symposium on Space Terahertz Technology, pp. 408-418, Ann Arbor,  
MI, March 24-26, 1992.
  
- [11] J.C. Swilhart, "Field solution for a thin film superconducting strip transmission  
line," J. Appl. Phys., vol. 32, pp 461-469, 1961.
  
- [12] T.R. Gheewala, "Design of 2.5-micrometer Josephson current injection logic," IBM  
J. Res. Develop., vol. 24, pp 130-142, 1980.

- [13] W.M. Chang, "The inductance of a superconducting strip transmission line," J. Appl. Phys., vol. 50, pp 8129-8134, 1979.
- [14] H.H.S. Javadi, W.R. McGrath, B. Bumble, and H.G. LeDuc, "Dispersion in Nb microstrip transmission lines at submillimeter wave frequencies," Appl. Phys. Lett., vol. 61, pp 2712-2714, 1992.
- [15] P. Febvre, W.R. McGrath, P. Batelaan, H.G. LeDuc, B. Bumble, M.A. Frerking, J. Hernichèl, "A 547 GHz SIS receiver employing a submicron Nb junction with an integrated matching circuit," Digest of the IEEE MTT-S International Microwave Symposium, Atlanta, June 14-18, 1993.
- [16] H.M. Pickett, J.C. Hardy, J. Farhoomand, "Characterization of a dual-mode horn for submillimeter wavelengths," IEEE Trans. Microwave Theory Tech., vol. MTT-32, pp 936, 1984.

[ 1 7 ] Made by Radiometer Physics, Meckenheim, Germany

- [18] K. Jacobs, U. Kotthaus, "Performance of a 230 GHz SIS receiver using Broadband Integrated Matching Structures," Conf. Digest of the 17th Int'l Conf. on IR and mm Waves, pp. 332-333, California Institute of Technology, Pasadena, California, December 14-17, 1992.
- [19] R.E. Eck, D.J. Scalapino and B.N. Taylor, "Self-detection of the ac Josephson current," Phys. Rev. Lett., vol. 13, No 1, pp. 15-18, July 1964.

- [20] A.V. Raisanen, W.R. McGrath, P. L. Richards and F.L. Lloyd, "Broad-band rf match to a millimeter-wave SIS quasi-particle mixer, " IEEE Trans. Microwave Theory Tech., vol. MIT-33, pp 1495-1500, 1985
- [21] P. Fcautrier, M. Hanus and P. Febvre, "Nb/Al-AlOx/Nb junctions for a 380 GHz SIS Receiver," Supercond. Sci. Tech nol., vol. 5, pp. 564-568, 1992.

## FIGURE CAPTIONS

Figure 1: SIS tunnel junction with an integrated parallel microstrip tuning circuit.

(a) Top view showing transmission line dimensions for 550 GHz/630 GHz.

(b) Cross section view showing film topology

Figure 2: Block diagram of SIS heterodyne receiver. Noise measurements are referred to the reference plane at the signal input port of the diplexer

Figure 3: Receiver noise temperature as a function of the LO frequency for 3 different SIS junctions. Junction O ( $R_N = 98 \Omega$ ) with no integrated RF tuning circuit gives the performance of the receiver with no additional compensation of the junction capacitance. The noise temperature varies from 850 K to 1150 K in the range 470-550 GHz. Junction A ( $R_N = 63 \Omega$ ) uses a parallel circuit with a radial stub optimized for 550 GHz while junction B ( $R_N = 73 \Omega$ ) has a tuning circuit designed for 630 GHz. Very good performance is obtained from 463 GHz to 635 GHz, with the best result  $T_R = 200$  K at 540 GHz for junction A and  $T_R = 362$  K at 626 GHz for junction B. The IF is 1.4 GHz and the bandwidth for noise measurements is 300 MHz.

Figure 4: Current vs. voltage characteristic (solid lines) for junction A with and without LO power applied at 540 GHz. Receiver IF output power,  $P_{IF}$  (dashed lines) for broadband hot and cold load signals at the RF input.

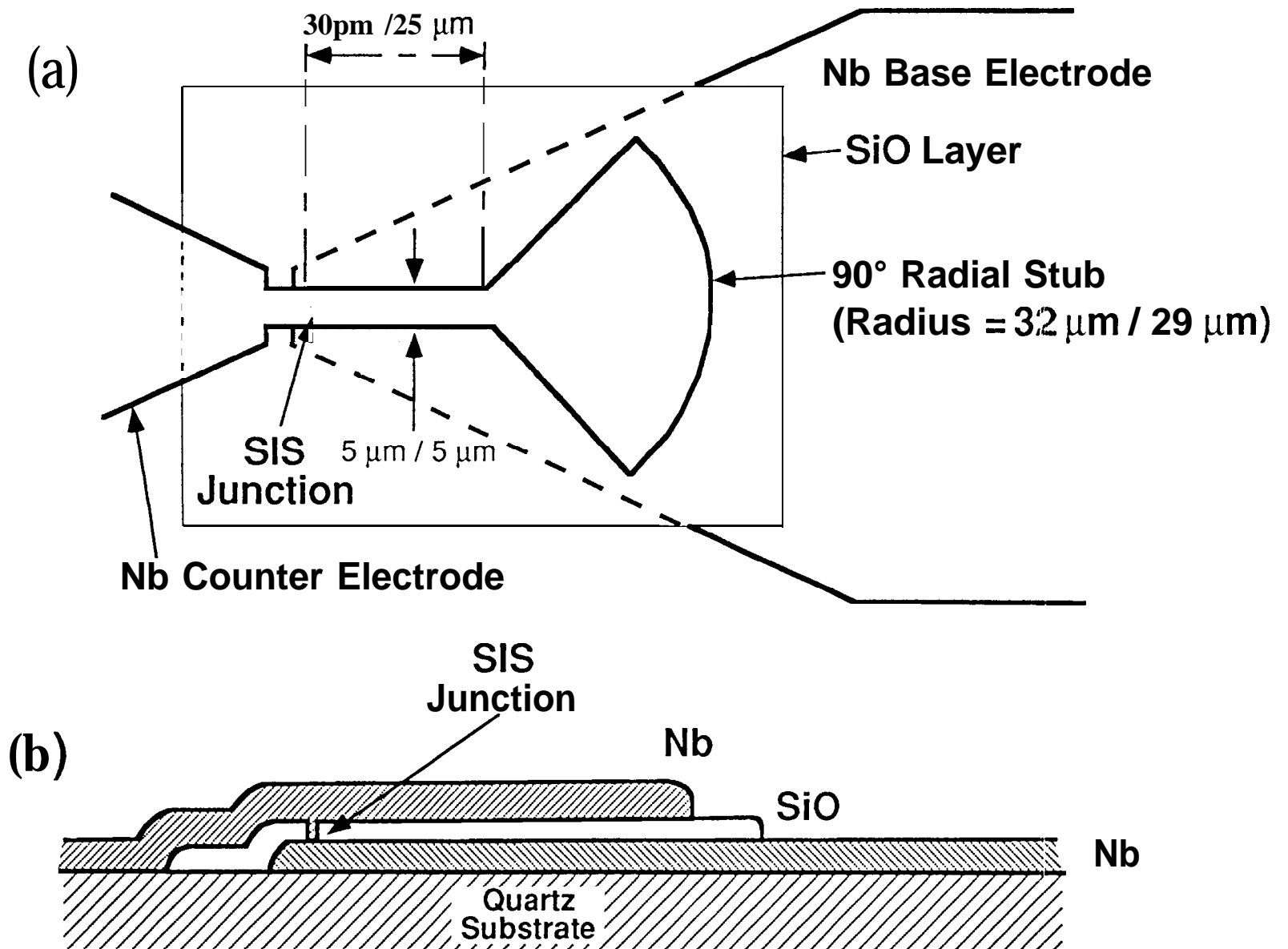


Fig. 1



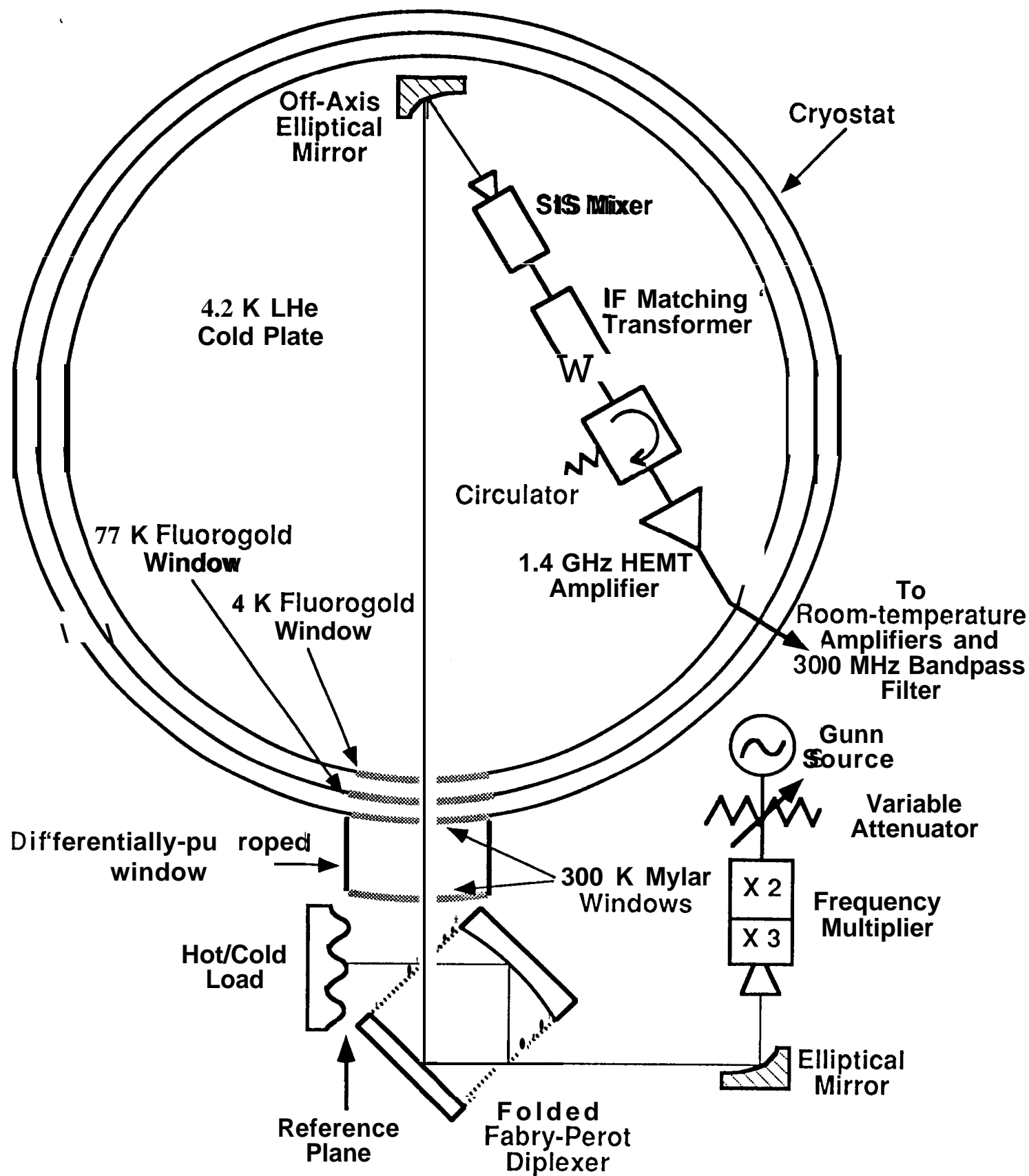


Fig. 2

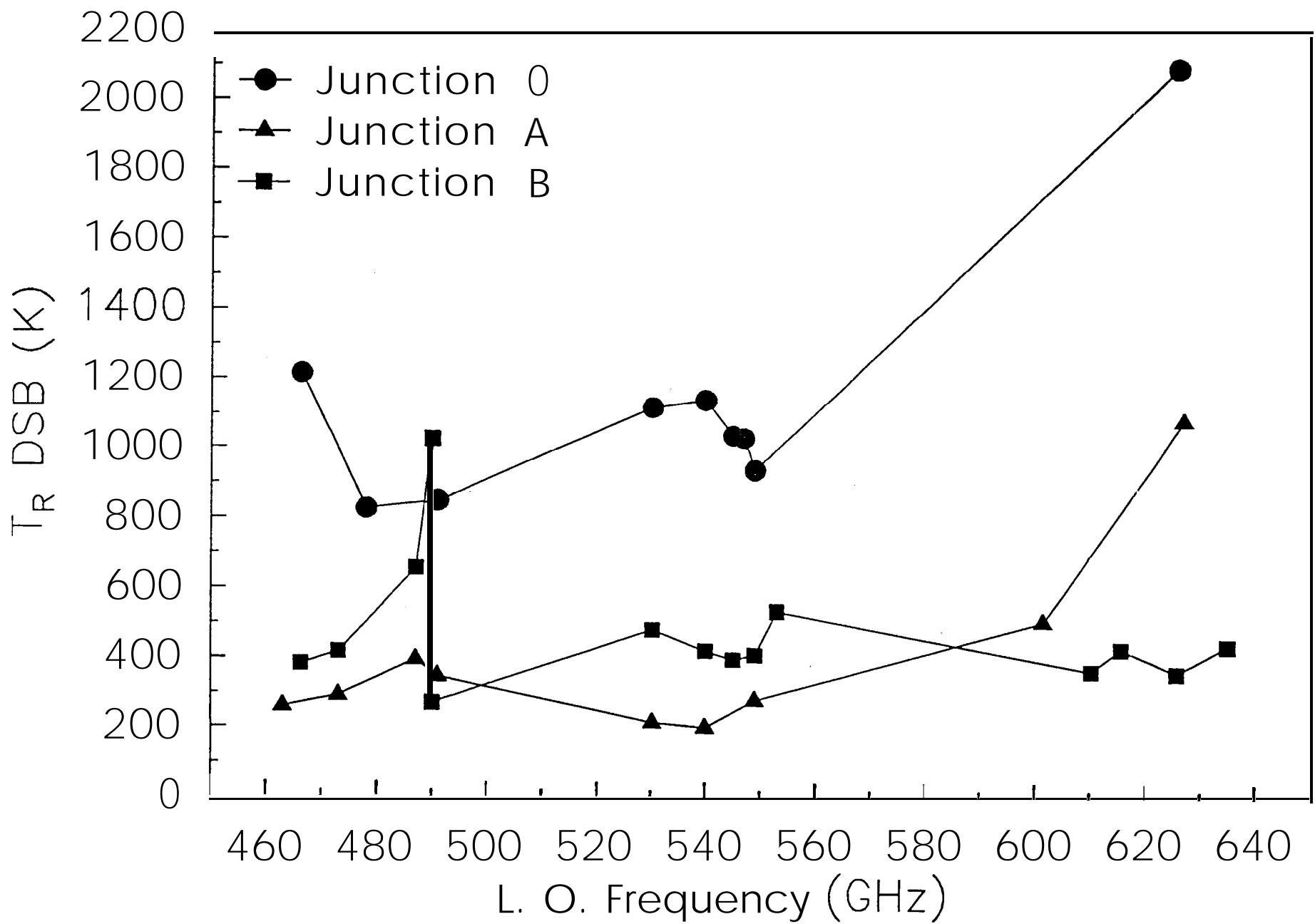


Fig. 3

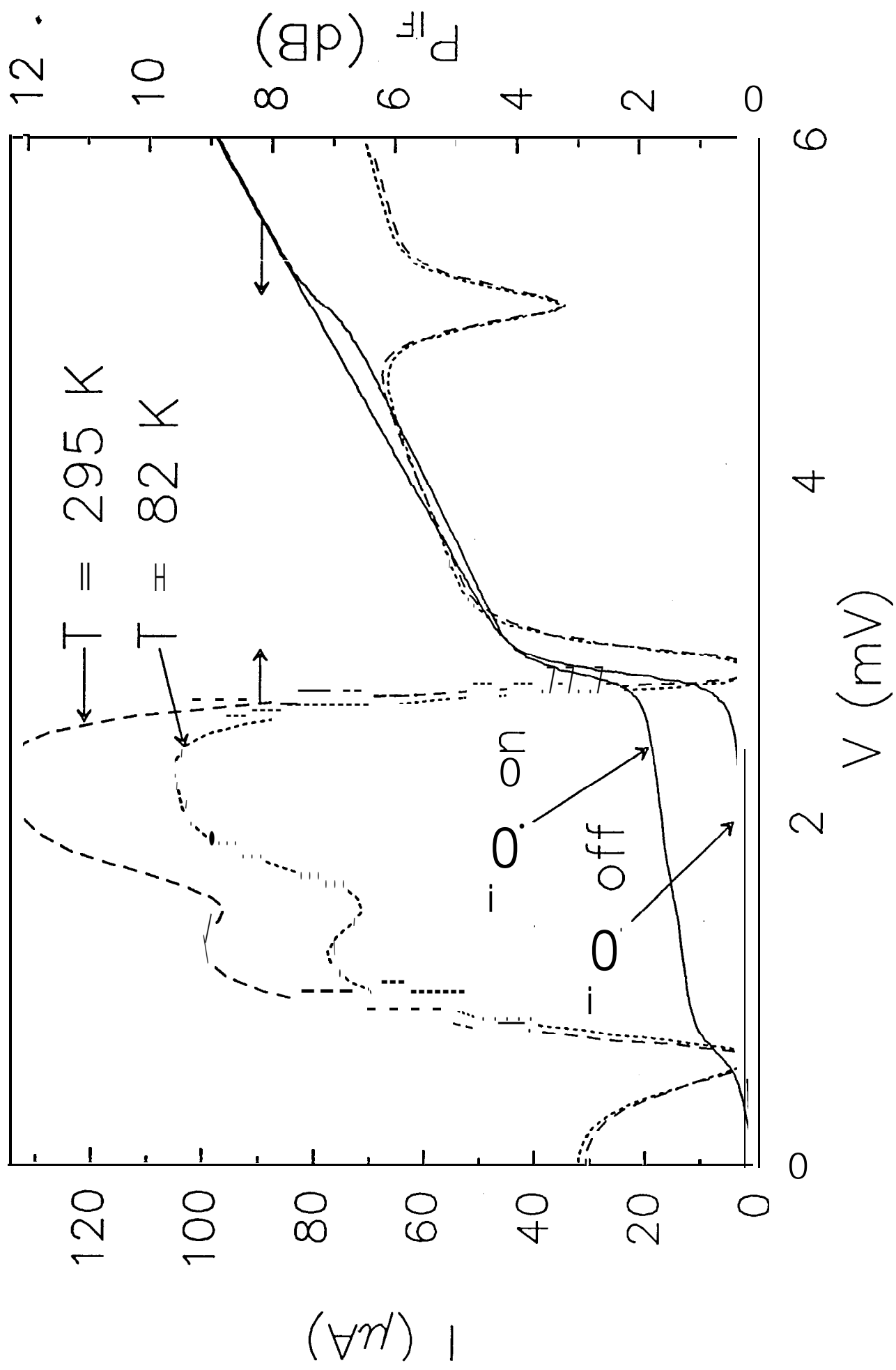


Fig. 4